

Exfoliated hexagonal BN as gate dielectric for InSb nanowire quantum dots with improved gate hysteresis and charge noise

Felix Jekat,¹ Benjamin Pestka,¹ Diana Car,² Saša Gazibegović,² Kilian Flöhr,¹ Sebastian Heedt,^{3, a)} Jürgen Schubert,³ Marcus Liebmann,¹ Erik P. A. M. Bakkers,² Thomas Schäpers,³ and Markus Morgenstern^{1, b)}

¹⁾*II. Institute of Physics B, RWTH Aachen University and JARA-FIT, 52074 Aachen, Germany*

²⁾*Department of Applied Physics, Eindhoven University of Technology, 5600 MB Eindhoven, The Netherlands*

³⁾*Peter Grünberg Institut (PGI-9) and JARA-FIT, Forschungszentrum Jülich, 52425 Jülich, Germany*

(Dated: June 12, 2022)

We characterize InSb quantum dots induced by bottom finger gates within a nanowire that is grown via the vapor-liquid-solid process. The gates are separated from the nanowire by an exfoliated 35 nm thin hexagonal BN flake. We probe the Coulomb diamonds of the gate induced quantum dot exhibiting charging energies of ~ 2.5 meV and orbital excitation energies up to 0.3 meV. The gate hysteresis for sweeps covering 5 Coulomb diamonds reveals an energy hysteresis of only 60 μ eV between upwards and downwards sweeps. Charge noise is studied via long-term measurements at the slope of a Coulomb peak revealing potential fluctuations of less than $3.6 \mu\text{eV}/\sqrt{\text{Hz}}$ at ~ 0.1 Hz. This makes h-BN the dielectric with the currently lowest gate hysteresis and lowest low-frequency potential fluctuations reported for low-gap III-V nanowires. The extracted values are similar to state-of-the-art quantum dots within Si/SiGe and Si/SiO₂ systems.

Recently, nanowires of indium antimonide (InSb) and indium arsenide (InAs)^{1–4} came back into focus due to their large spin-orbit coupling^{5–7} that in combination with magnetic fields and a relatively strong proximity-induced superconductivity^{8–10} enables tuning of Majorana modes^{11–14} as a basis for topologically protected quantum computing.^{15–17} Typically, the nanowires are tuned electrically by a number of bottom finger gates that are separated from the nanowire by a gate dielectric.^{12,18} It is well known that both charge noise and hysteresis of gate-induced potentials deteriorate the performance of semiconductor qubits,^{19–22} as is also expected for the prospective Majorana qubits.^{23,24} Hence, it is crucial to optimize the dielectric in terms of unintentional charge fluctuations.

For exfoliated two-dimensional materials such as graphene, it turned out that hexagonal boron nitride (h-BN) is ideal for that purpose.^{25,26} For example, it improves the charge carrier mobility by more than an order of magnitude compared to the previously used Si/SiO₂.^{27,28} Furthermore, it is easy to fabricate. Thus, exploiting exfoliated h-BN as gate dielectric for low-gap III-V nanowires is appealing. First experiments used h-BN to separate the global Si/SiO₂ back gate from an InSb nanowire enabling the first quantized conductance steps in such nanowires at zero magnetic field.²⁹ Subsequently, measurements on proximity-coupled InSb nanowires on h-BN showed magnetic field induced zero bias peaks, indicative of the presence of Majorana zero modes.^{30,31} However, Coulomb diamonds with excited states in a gate-induced quantum dot have not been reported and, more importantly, the charge noise and gate hysteresis of such nanowires on h-BN have not been studied. Reports on these properties are only available for other types of dielectrics.^{32–42} They ex-

hibit, e.g., a relatively large low-temperature gate hysteresis on LaLuO₃ and SiO₂ being 0.5 V and 2 V at gate sweeps of 4 V and 30 V, respectively.^{41,42} Noise properties for quantum dots have only been reported for a vacuum dielectric revealing $1/f$ behavior above ~ 300 Hz and an upturn at lower frequency with noise of $\sim 0.2 \mu\text{eV}/\sqrt{\text{Hz}}$ at 100 Hz.³³

Here, we study an InSb nanowire/h-BN device with bottom finger gates (pitch 90 nm) at the temperature $T = 300$ mK. The device exhibits a gate hysteresis of 2 mV for sweeps of 150 mV (250 mV) at a rate of 25 mV/s (42 mV/h), hence, significantly better than in previous reports.^{41,42} It, moreover, shows a charge noise of only $3.6 \mu\text{eV}/\sqrt{\text{Hz}}$ at 0.1 Hz with an approximate $1/f^{1.5}$ dependence towards lower frequencies. The noise is likely even less than for the previously studied vacuum dielectric³³ pointing to remaining limitations due to defects at the nanowire itself. More importantly, the values are similar to state-of-the-art quantum dots in Si/SiGe or Si/SiO₂ structures ($\sim 3 \mu\text{eV}/\sqrt{\text{Hz}}$ at 1 Hz).^{22,43–45} Hence, h-BN turns out to be a favorable dielectric for low-gap III-V nanowires.

The InSb nanowires were grown on top of InP stems via the vapor-liquid-solid (VLS) method using a gold droplet as catalyst.^{46,47} A quantum dot device of such a nanowire (Fig. 1(a)–(b)) consists of a 200 nm thick SiN_x layer, on a highly doped Si substrate acting as a global back gate (BG) with multiple finger gates made (G1–G4, FG) on top. The finger gates are 35 nm wide and defined by electron beam lithography (EBL) with a spacing of 55 nm except between G3 and FG where the spacing is 130 nm. An h-BN flake is deposited on top of the finger gates via the dry transfer method.²⁷ Subsequently, one InSb nanowire is placed onto the h-BN with sub- μm lateral precision via an indium tip attached to a micromanipulator.⁴⁸ Finally, source and drain contacts are prepared via EBL. Prior to the metal deposition of the Ti/Au (10 nm/110 nm) contacts, the exposed nanowire area is passivated ex-situ by sulphur⁴⁹ and subsequently cleaned in-situ by argon ion bombardment. Transport measurements are performed at $T = 300$ mK in a ³He magneto-cryostat (Teslatron

^{a)}Current address: Microsoft Quantum Lab Delft, 2600 GA Delft, The Netherlands

^{b)}mmorgens@physik.rwth-aachen.de

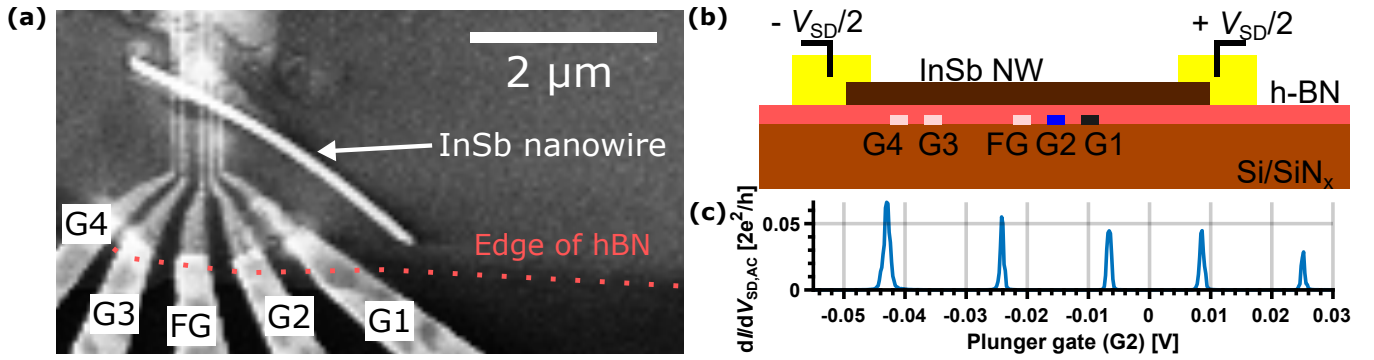


Figure 1. (a) Scanning electron microscopy image of the device prior to depositing source and drain contacts. Different finger gates (G1-G4) and a floating gate (FG) are labeled. Nanowire diameter: ~ 100 nm. (b) Side view sketch of the device. Si/SiN_x (light brown) acts as a global backgate (BG). Finger gates G1-G4 and FG (white, blue, black) are deposited on top and buried below a 35 nm thick h-BN flake (pink). The nanowire (dark brown) is contacted by two Ti/Au pads (yellow) at distance 2.2 μm used to apply the source-drain voltage V_{SD} . Light brown, blue and black colors of gates match the colors of the corresponding phase stability diagrams in Fig. 2, where these gates are used as plunger gate. (c) Nanowire conductance $dI/dV_{SD,AC}$ as a function of the voltage V_{G2} at gate G2. Coulomb peaks appear due to the formation of a quantum dot confined by energy barriers that are induced via G1 and G3, $V_{G1} = -650$ mV, $V_{G3} = -980$ mV, $V_{BG} = 3$ V, $V_{SD,AC} = 20$ μV, $f_{AC} = 83$ Hz, $V_{SD,DC} = 0$ V, $T = 300$ mK.

from Oxford Instruments). Before cool-down, the insert is evacuated to 10^{-6} mbar for 48 h at 300 K in order to remove adsorbates from the nanowire surface.⁴²

Gate dependent conductivity traces (not shown) reveal a low temperature mobility of the nanowire of $\mu = 28000$ cm²/Vs.⁴² Using the finger gates, we induce a quantum dot within the nanowire exhibiting regularly spaced Coulomb peaks (Fig. 1(c)). Different combinations of finger gates can be used to obtain charge stability diagrams of such quantum dots (Fig. 2(a)-(c)). Besides regularly spaced Coulomb diamonds for all combinations of gates, excited states are visible at larger V_{SD} . Only very few perturbations appear, that are likely caused by uncontrolled charging events in the surrounding of the quantum dot. For the gate configurations of Fig. 2(a)-(c), one straightforwardly deduces charging energies E_C up to 3 meV, 2.3 meV, and 2.5 meV, respectively, excitation energies Δ of ~ 0.5 meV, 0.3 meV, and 0.2 – 1 meV, respectively, and lever arms α of 0.05 eV/V, 0.12 eV/V, and 0.03 eV/V, respectively.

To quantify the charge noise acting on the nanowire quantum dot, Fig. 3(a) shows low-frequency noise measurements recorded at 300 mK. We measure the temporal current fluctuations at the slope of a Coulomb peak for $V_{SD,DC} = 40$ μV. In order to transfer this to the potential fluctuation noise $S_{pot}(f)$ as function of frequency f , we firstly use the measured shape of the Coulomb peak in $I(V_{G2})$ traces, well fitted by a Fermi-Dirac peak, to deduce the gate voltage noise. Then, we transfer gate voltage to potential energy via $\alpha = 0.04$ eV/V as deduced from the respective Coulomb diamond. The square root of the power spectral density of the resulting temporal potential fluctuations in the quantum dot leads to $S_{pot}(f)$ in eV/ $\sqrt{\text{Hz}}$ (Fig. 3(a), blue trace). It is $S_{pot}(0.1 \text{ Hz}) = 3.6$ μeV/ $\sqrt{\text{Hz}}$ and increases towards lower f mostly following $S_{pot}^2(f) \propto 1/f^{1.5}$ (red fit line). The enhanced logarithmic slope of $S_{pot}^2(f)$ with respect to the classical $1/f$ noise is in reasonable agreement with the upturn of the $1/f$ noise below $f = 100$ Hz observed

earlier for InAs nanowires with vacuum dielectric³³. For comparison, we also investigated an InAs nanowire⁵⁰ on a LaLuO₃ dielectric in the same frequency range. Except for the dielectric, deposited via pulsed laser deposition⁴¹, the device is prepared in the same way as the InSb nanowire device on h-BN. The displayed $S_{pot}(f)$ (Fig. 3(a), orange trace) originates from temporal current measurements at the pinch-off of the nanowire using a single finger gate. It is, hence, converted to $S_{pot}(f)$ again by the measured $I(V_{G1})$ but then using $\alpha = 0.1$ eV/V as deduced from the geometry of the sample. Remarkably, $S_{pot}(f)$ of the h-BN device is three orders of magnitude lower than for the LaLuO₃ device (Fig. 3(a)).

Comparison with literature data on noise for III-V low-gap nanowires is difficult. Either much longer parts of the nanowire are gated³², effectively averaging charge fluctuations, or the frequencies are significantly larger due to probing by radio frequency via reflection at the quantum dot.³³ Since $S_{pot}^2(f)$ is steeper than $1/f$ at low frequency, an extrapolation is not reliable. However, conservatively extrapolating the noise data obtained for the suspended InAs nanowire (vacuum dielectric) at 100 Hz³³ towards 0.1 Hz by a $1/f$ curve reveals $S_{pot}(0.1 \text{ Hz}) \simeq 5$ μeV/ $\sqrt{\text{Hz}}$. This is larger than for our device on h-BN, albeit vacuum without defects has been used as dielectric. It strongly suggests that the major charge noise in both cases originates from charge traps within or on the nanowire and not from the dielectric. It is instructive to compare our data with the charge noise in Si or Si/SiGe quantum dots^{22,43-45}, currently considered as most promising for semiconductor spin qubits⁵¹. For these quantum dots, one finds $S_{pot}^2(f \simeq 1 \text{ Hz}) \propto 1/f^\beta$ with device-dependent $\beta = 1 - 1.4$ and, consistently, an increase of $S_{pot}(f)$ with increasing T . Favorably, the reported $S_{pot}(f)$ at 0.3 K (2-5 μeV/ $\sqrt{\text{Hz}}$ at 1 Hz)⁴³⁻⁴⁵ are quite similar to our InSb nanowire quantum dot on h-BN (3.6 μeV/ $\sqrt{\text{Hz}}$ at 0.1 Hz). This renders the device competitive to the most favorable material combinations in terms of charge noise.

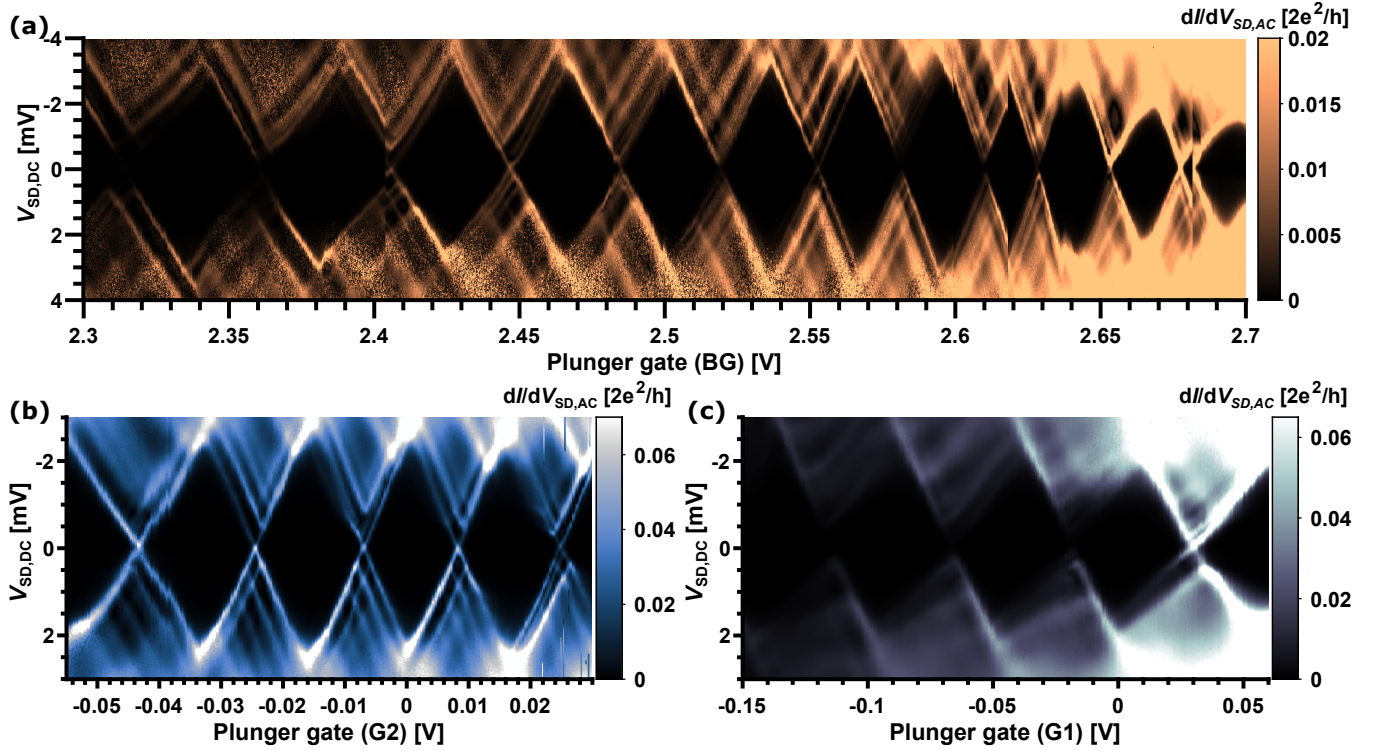


Figure 2. Charge stability diagrams of different quantum dots in the same InSb nanowire using different combinations of finger gates. Fast scan direction is along $V_{SD,DC}$, $V_{SD,AC} = 20 \mu\text{V}$, $f_{AC} = 83 \text{ Hz}$, $V_{G4} = 0 \text{ V}$, $T = 300 \text{ mK}$. (a) Quantum dot confined by G2 and G3 and charged by BG, $V_{G2} = -700 \text{ mV}$, $V_{G3} = -1 \text{ V}$, $V_{G1} = 0 \text{ V}$. A few perturbations are visible at $V_{BG} = 2.68 \text{ V}$, 2.64 V , 2.62 V and 2.6 V , likely due to uncontrolled charging events during the early stages of the measurement. (b) Quantum dot confined by G1 and G3 and charged by G2, $V_{G1} = -650 \text{ mV}$, $V_{G3} = -980 \text{ mV}$, $V_{BG} = 3 \text{ V}$. (c) Quantum dot confined by G2 and G3 and charged by G1, $V_{G2} = -580 \text{ mV}$, $V_{G3} = -922 \text{ mV}$, $V_{BG} = 3 \text{ V}$.

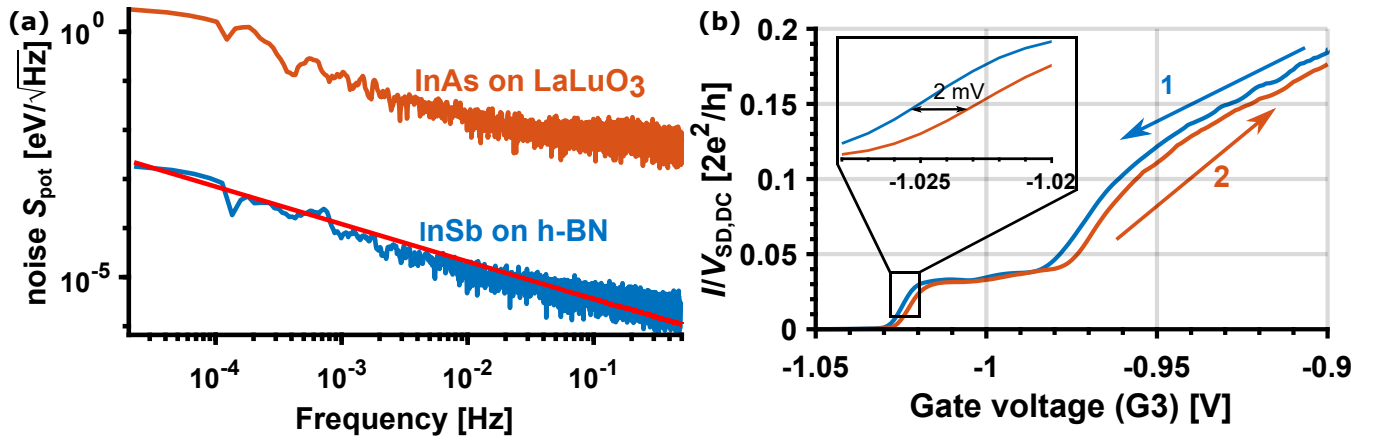


Figure 3. (a) Frequency dependent potential fluctuation noise $S_{pot}(f)$ of an InSb nanowire quantum dot on h-BN dielectric (blue) with fit curve (red). The noise is deduced from the current noise observed at a gate voltage tuned to the slope of a Coulomb peak (see text), $V_{G1} = 70 \text{ mV}$, $V_{G2} = -560 \text{ mV}$, $V_{G3} = -890 \text{ mV}$, $V_{BG} = 3 \text{ V}$, $V_{SD,DC} = 40 \mu\text{V}$, $V_{SD,AC} = 20 \mu\text{V}$, $f_{AC} = 83 \text{ Hz}$. For comparison, $S_{pot}(f)$ of an InAs nanowire on LaLuO₃ dielectric (orange) is shown, $V_{SD,DC} = 5 \text{ mV}$, $V_{SD,AC} = 20 \mu\text{V}$, $f_{AC} = 1.1 \text{ kHz}$, $V_{G1} = -10 \text{ V}$, all other gates grounded. Both devices are fabricated using the same deposition methods except for the dielectric. (b) V_{G3} dependent conductance curves of the InSb nanowire on h-BN close to pinch-off (without inducing a quantum dot). Arrows with numbers indicate the subsequent sweep directions of V_{G3} . Inset: zoom showing a hysteresis of $\sim 2 \text{ mV}$, sweep rate: 25 mV/s , $V_{SD,DC} = 3 \text{ mV}$, $V_{SD,AC} = 20 \mu\text{V}$, $f_{AC} = 83 \text{ Hz}$, $V_{BG} = 3 \text{ V}$, all other gates grounded. (a), (b) $T = 300 \text{ mK}$.

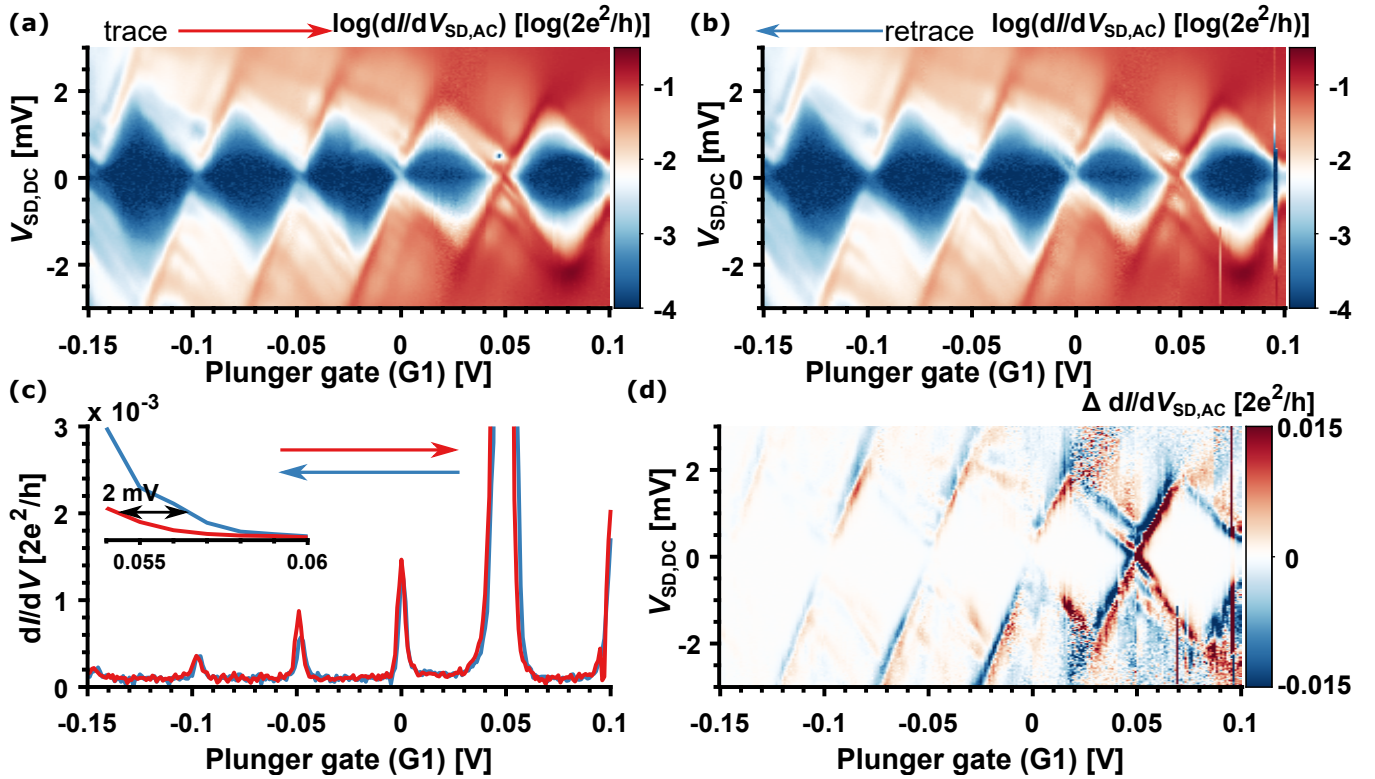


Figure 4. (a), (b) Charge stability diagrams for a quantum dot confined by gates G2 and G3 and charged by gate G1. The two diagrams are recorded directly after each other with different gate sweep directions as marked by arrows on top. Fast sweep direction is along $V_{SD,DC}$, total measurement time: 12 h, gate sweep rate: 42 mV/h. (c) Line cut through (a) (red) and (b) (blue) at $V_{SD,DC} = 0$ mV. Inset: zoom with marked hysteresis of 2 mV. (d) Difference of the data of (b) and (a). Parameters: $V_{G2} = -580$ mV, $V_{G3} = -922$ mV, $V_{BG} = 3$ V, $V_{SD,AC} = 20$ μ V, $f_{AC} = 83$ Hz, $T = 300$ mK.

The second important benchmark for a dielectric is the gate hysteresis. Figure 3(b) reveals that the InSb nanowire on h-BN exhibits a gate hysteresis $\Delta V_{\text{hyst}} \simeq 2$ mV (inset) at a sweep rate of 25 mV/s. For the gate range $\Delta V_{\text{gate}} = 150$ mV, this leads to a ratio $R = \Delta V_{\text{hyst}}/\Delta V_{\text{gate}} = 0.013$, much lower than observed previously for InAs or InSb nanowires on other gate dielectrics: $R = 0.13^{41}$, $R = 0.07^{42}$. Since R typically depends on the sweep rate^{52,53}, we improved it further by reducing the gate sweep rate to 42 mV/h leading to $R = 0.008$ with $\Delta V_{\text{gate}} = 250$ mV. The extremely low rate is employed to record full charge stability diagrams subsequently for both gate sweep directions (Fig. 4(a),(b)). The total measurement time of 12 h evidences the long term stability of the quantum dot by the excellent similarity of the two diagrams. Only two conductivity jumps (Fig. 4(b), right) are observed. The gate hysteresis is quantified by a line cut at $V_{SD} = 0$ mV (Fig. 4(c)) revealing $\Delta V_{\text{hyst}} = 2$ mV as maximum hysteresis between the two curves (inset) and, hence, implying $R = 0.008$. Using $\alpha = 0.03$ eV/V, one can calculate the energy hysteresis $\Delta E = 60$ μ eV. Figure 4(d) displays the difference between Fig. 4(b) and Fig. 4(a) showing that the small hysteresis is reliably observed across the whole charge stability diagram. The observation of a small hysteresis, low charge noise and a small number of jumps in stability diagrams consistently indicate a very low number of chargeable impurities in the h-BN

layer, thus making it a favorable dielectric for III-V nanowire devices. As pointed out above, the performance is likely limited by the remaining charge traps on the nanowire itself.

In summary, we have presented an InSb nanowire device with an h-BN flake as gate dielectric. With a set of finger gates, electrons are confined in quantum dots using different gate configurations, resulting in regular Coulomb diamonds with multiple excited states. Favorably, the device has the lowest noise level (3.6 μ eV/ $\sqrt{\text{Hz}}$ at ~ 0.1 Hz) reported for low-gap III-V nanowire devices yet and shows an unprecedented gate hysteresis of 2 mV only. Hence, in terms of charge noise, h-BN is the currently most favorable dielectric for low-gap III-V nanowire devices.

ACKNOWLEDGMENTS

We thank Stefan Trelenkamp and Florian Lenz for help with the EBL and acknowledge helpful discussions with Hendrik Bluhm. Funding by the Deutsche Forschungsgemeinschaft (DFG, German Research Foundation) under Germany's Excellence Strategy – Cluster of Excellence Matter and Light for Quantum Computing (ML4Q) EXC 2004/1 – 390534769 and by European Graphene Flagship Core 2, grant number 785219 is gratefully acknowledged.

REFERENCES

- ¹K. Hiruma, M. Yazawa, T. Katsuyama, K. Ogawa, K. Haraguchi, M. Koguchi, and H. Kakibayashi, "Growth and optical properties of nanometer-scale GaAs and InAs whiskers," *J. Appl. Phys.* **77**, 447–462 (1995).
- ²L. E. Jensen, M. T. Björk, S. Jeppesen, A. I. Persson, B. J. Ohlsson, and L. Samuelson, "Role of surface diffusion in chemical beam epitaxy of InAs nanowires," *Nano Lett.* **4**, 1961–1964 (2004).
- ³M. T. Björk, B. J. Ohlsson, C. Thelander, A. I. Persson, K. Deppert, L. R. Wallenberg, and L. Samuelson, "Nanowire resonant tunneling diodes," *Appl. Phys. Lett.* **81**, 4458–4460 (2002).
- ⁴B. M. Borg and L.-E. Wernersson, "Synthesis and properties of antimonide nanowires," *Nanotechnology* **24**, 202001 (2013).
- ⁵H. A. Nilsson, P. Caroff, C. Thelander, M. Larsson, J. B. Wagner, L.-E. Wernersson, L. Samuelson, and H. Q. Xu, "Giant, level-Dependent Factors in InSb nanowire quantum dots," *Nano Lett.* **9**, 3151–3156 (2009).
- ⁶S. Nadj-Perge, S. M. Frolov, E. P. A. M. Bakkers, and L. P. Kouwenhoven, "Spin-orbit qubit in a semiconductor nanowire," *Nature* **468**, 1084–1087 (2010).
- ⁷C. Fasth, A. Fuhrer, L. Samuelson, V. N. Golovach, and D. Loss, "Direct measurement of the spin-orbit interaction in a two-electron InAs nanowire quantum dot," *Phys. Rev. Lett.* **98**, 266801 (2007).
- ⁸Y.-J. Doh, "Tunable supercurrent through semiconductor nanowires," *Science* **309**, 272–275 (2005).
- ⁹H. Takayanagi and T. Kawakami, "Superconducting proximity effect in the native inversion layer on InAs," *Phys. Rev. Lett.* **54**, 2449–2452 (1985).
- ¹⁰H. A. Nilsson, P. Samuelsson, P. Caroff, and H. Q. Xu, "Supercurrent and multiple andreev reflections in an InSb nanowire josephson junction," *Nano Lett.* **12**, 228–233 (2012).
- ¹¹J. Alicea, "New directions in the pursuit of majorana fermions in solid state systems," *Rep. Prog. Phys.* **75**, 076501 (2012).
- ¹²V. Mourik, K. Zuo, S. M. Frolov, S. R. Plissard, E. P. A. M. Bakkers, and L. P. Kouwenhoven, "Signatures of majorana fermions in hybrid superconductor-semiconductor nanowire devices," *Science* **336**, 1003–1007 (2012).
- ¹³S. M. Albrecht, A. P. Higginbotham, M. Madsen, F. Kuemmeth, T. S. Jespersen, J. Nygård, P. Krogstrup, and C. M. Marcus, "Exponential protection of zero modes in majorana islands," *Nature* **531**, 206–209 (2016).
- ¹⁴R. M. Lutchyn, E. P. A. M. Bakkers, L. P. Kouwenhoven, P. Krogstrup, C. M. Marcus, and Y. Oreg, "Majorana zero modes in superconductor-semiconductor heterostructures," *Nat. Rev. Mater.* **3**, 52–68 (2018).
- ¹⁵A. Stern and N. H. Lindner, "Topological quantum computation—from basic concepts to first experiments," *Science* **339**, 1179–1184 (2013).
- ¹⁶S. Vijay, T. H. Hsieh, and L. Fu, "Majorana fermion surface code for universal quantum computation," *Phys. Rev. X* **5**, 041038 (2015).
- ¹⁷D. Litinski, M. S. Kesselring, J. Eisert, and F. von Oppen, "Combining topological hardware and topological software: Color-code quantum computing with topological superconductor networks," *Phys. Rev. X* **7**, 031048 (2017).
- ¹⁸A. Das, Y. Ronen, Y. Most, Y. Oreg, M. Heiblum, and H. Shtrikman, "Zero-bias peaks and splitting in an al-InAs nanowire topological superconductor as a signature of majorana fermions," *Nat. Phys.* **8**, 887–895 (2012).
- ¹⁹D. Culcer, X. Hu, and S. D. Sarma, "Dephasing of si spin qubits due to charge noise," *Appl. Phys. Lett.* **95**, 073102 (2009).
- ²⁰A. V. Kuhlmann, J. Houel, A. Ludwig, L. Greuter, D. Reuter, A. D. Wieck, M. Poggio, and R. J. Warburton, "Charge noise and spin noise in a semiconductor quantum device," *Nat. Phys.* **9**, 570–575 (2013).
- ²¹J. Yoneda, K. Takeda, T. Otsuka, T. Nakajima, M. R. Delbecq, G. Allison, T. Honda, T. Koderu, S. Oda, Y. Hoshi, N. Usami, K. M. Itoh, and S. Tarucha, "A quantum-dot spin qubit with coherence limited by charge noise and fidelity higher than 99.9%," *Nat. Nanotechnol.* **13**, 102–106 (2017).
- ²²X. Mi, S. Kohler, and J. R. Petta, "Landau-zener interferometry of valley-orbit states in si/SiGe double quantum dots," *Phys. Rev. B* **98**, 161404 (2018).
- ²³M. J. Schmidt, D. Rainis, and D. Loss, "Decoherence of majorana qubits by noisy gates," *Phys. Rev. B* **86**, 085414 (2012).
- ²⁴T. Li, W. A. Coish, M. Hell, K. Flensberg, and M. Leijnse, "Four-majorana qubit with charge readout: Dynamics and decoherence," *Phys. Rev. B* **98**, 205403 (2018).
- ²⁵A. K. Geim and I. V. Grigorieva, "Van der waals heterostructures," *Nature* **499**, 419–425 (2013).
- ²⁶R. Frisenda, E. Navarro-Moratalla, P. Gant, D. P. D. Lara, P. Jarillo-Herrero, R. V. Gorbachev, and A. Castellanos-Gomez, "Recent progress in the assembly of nanodevices and van der waals heterostructures by deterministic placement of 2d materials," *Chem. Soc. Rev.* **47**, 53–68 (2018).
- ²⁷C. R. Dean, A. F. Young, I. Meric, C. Lee, L. Wang, S. Sorgenfrei, K. Watanabe, T. Taniguchi, P. Kim, K. L. Shepard, and J. Hone, "Boron nitride substrates for high-quality graphene electronics," *Nat. Nanotechnol.* **5**, 722–726 (2010).
- ²⁸L. Banszerus, M. Schmitz, S. Engels, M. Goldsche, K. Watanabe, T. Taniguchi, B. Beschoten, and C. Stampfer, "Ballistic transport exceeding 28 μm in CVD grown graphene," *Nano Lett.* **16**, 1387–1391 (2016).
- ²⁹J. Kammhuber, M. C. Cassidy, H. Zhang, Ö. Gül, F. Pei, M. W. A. de Moor, B. Nijholt, K. Watanabe, T. Taniguchi, D. Car, S. R. Plissard, E. P. A. M. Bakkers, and L. P. Kouwenhoven, "Conductance quantization at zero magnetic field in InSb nanowires," *Nano Lett.* **16**, 3482–3486 (2016).
- ³⁰Ö. Gül, H. Zhang, J. D. S. Bommer, M. W. A. de Moor, D. Car, S. R. Plissard, E. P. A. M. Bakkers, A. Geresdi, K. Watanabe, T. Taniguchi, and L. P. Kouwenhoven, "Ballistic majorana nanowire devices," *Nat. Nanotechnol.* **13**, 192–197 (2018).
- ³¹S. T. Gill, J. Damasco, B. E. Janicek, M. S. Durkin, V. Humbert, S. Gazibegovic, D. Car, E. P. A. M. Bakkers, P. Y. Huang, and N. Mason, "Selective-area superconductor epitaxy to ballistic semiconductor nanowires," *Nano Lett.* **18**, 6121–6128 (2018).
- ³²M. R. Sakr and X. P. A. Gao, "Temperature dependence of the low frequency noise in indium arsenide nanowire transistors," *Appl. Phys. Lett.* **93**, 203503 (2008).
- ³³H. A. Nilsson, T. Duty, S. Abay, C. Wilson, J. B. Wagner, C. Thelander, P. Delsing, and L. Samuelson, "A radio frequency single-electron transistor based on an InAs/InP heterostructure nanowire," *Nano Lett.* **8**, 872–875 (2008).
- ³⁴C. J. Delker, S. Kim, M. Borg, L. Wernersson, and D. B. Janes, "1/f noise sources in dual-gated indium arsenide nanowire transistors," *IEEE T. Electron. Dev.* **59**, 1980–1987 (2012).
- ³⁵S. Vitusevich and I. Zadorozhnyi, "Noise spectroscopy of nanowire structures: fundamental limits and application aspects," *Semicond. Sci. Tech.* **32**, 043002 (2017).
- ³⁶C. J. Delker, Y. Zi, C. Yang, and D. B. Janes, "Low-frequency noise contributions from channel and contacts in InAs nanowire transistors," *IEEE T. Electron Dev.* **60**, 2900–2905 (2013).
- ³⁷M. Petrychuk, I. Zadorozhnyi, Y. Kutovyi, S. Karg, H. Riel, and S. Vitusevich, "Noise spectroscopy to study the 1d electron transport properties in InAs nanowires," *Nanotechnology* **30**, 305001 (2019).
- ³⁸K.-M. Persson, B. G. Malm, and L.-E. Wernersson, "Surface and core contribution to 1/f-noise in InAs nanowire metal-oxide-semiconductor field-effect transistors," *Appl. Phys. Lett.* **103**, 033508 (2013).
- ³⁹K.-M. Persson, E. Lind, A. W. Dey, C. Thelander, H. Sjolund, and L.-E. Wernersson, "Low-frequency noise in vertical InAs nanowire FETs," *IEEE Electr. Device L.* **31**, 428–430 (2010).
- ⁴⁰R. E. Wahl, F. Wang, H. E. Chung, G. R. Kunnen, S. Yip, E. H. Lee, E. Y. B. Pun, G. B. Raupp, D. R. Allee, and J. C. Ho, "Stability and low-frequency noise in InAs NW parallel-array thin-film transistors," *IEEE Electr. Device L.* **34**, 765–767 (2013).
- ⁴¹C. Volk, J. Schubert, M. Schnee, K. Weis, M. Akabori, K. Sladek, H. Hardt-degen, and Th. Schäfers, "LaLuO₃ as a high-k gate dielectric for InAs nanowire structures," *Semicond. Sci. Technol.* **25**, 085001 (2010).
- ⁴²Ö. Gül, D. J. van Woerkom, I. van Weperen, D. Car, S. R. Plissard, E. P. A. M. Bakkers, and L. P. Kouwenhoven, "Towards high mobility InSb nanowire devices," *Nanotechnology* **26**, 215202 (2015).
- ⁴³B. M. Freeman, J. S. Schoenfeld, and H. Jiang, "Comparison of low frequency charge noise in identically patterned Si/SiO₂ and Si/SiGe quantum dots," *Appl. Phys. Lett.* **108**, 253108 (2016).
- ⁴⁴L. Petit, J. Boter, H. Eenink, G. Droulers, M. Tagliaferri, R. Li, D. Franke, K. Singh, J. Clarke, R. Schouten, V. Dobrovitski, L. Vandersypen, and M. Veldhorst, "Spin lifetime and charge noise in hot silicon quantum dot qubits," *Phys. Rev. Lett.* **121**, 076801 (2018).
- ⁴⁵E. J. Connors, J. Nelson, H. Qiao, L. F. Edge, and J. M. Nichol, "Low-

- frequency charge noise in Si/SiGe quantum dots,” *Phys. Rev. B* **100**, 165305 (2019).
- ⁴⁶S. R. Plissard, D. R. Slapak, M. A. Verheijen, M. Hocevar, G. W. G. Immink, I. van Weperen, S. Nadj-Perge, S. M. Frolov, L. P. Kouwenhoven, and E. P. A. M. Bakkers, “From InSb nanowires to nanocubes: Looking for the sweet spot,” *Nano Lett.* **12**, 1794–1798 (2012).
- ⁴⁷D. Car, J. Wang, M. A. Verheijen, E. P. A. M. Bakkers, and S. R. Plissard, “Rationally designed single-crystalline nanowire networks,” *Adv. Mater.* **26**, 4875–4879 (2014).
- ⁴⁸K. Flöhr, M. Liebmann, K. Sladek, H. Y. Günel, R. Frielinghaus, F. Haas, C. Meyer, H. Hardtdegen, Th. Schäpers, D. Grützmacher, and M. Morgenstern, “Manipulating InAs nanowires with submicrometer precision,” *Rev. Sci. Instrum.* **82**, 113705 (2011).
- ⁴⁹D. B. Suyatin, C. Thelander, M. T. Björk, I. Maximov, and L. Samuelson, “Sulfur passivation for ohmic contact formation to InAs nanowires,” *Nanotechnology* **18**, 105307 (2007).
- ⁵⁰Q.-T. Do, K. Blekker, I. Regolin, W. Prost, and F.-J. Tegude, “High transconductance MISFET with a single InAs nanowire channel,” *IEEE Electr. Device L.* **28**, 682–684 (2007).
- ⁵¹T. F. Watson, S. G. J. Philips, E. Kawakami, D. R. Ward, P. Scarlino, M. Veldhorst, D. E. Savage, M. G. Lagally, M. Friesen, S. N. Coppersmith, M. A. Eriksson, and L. M. K. Vandersypen, “A programmable two-qubit quantum processor in silicon,” *Nature* **555**, 633–637 (2018).
- ⁵²D. Lynall, S. V. Nair, D. Gutstein, A. Shik, I. G. Savelyev, M. Blumin, and H. E. Ruda, “Surface state dynamics dictating transport in InAs nanowires,” *Nano Lett.* **18**, 1387–1395 (2018).
- ⁵³S. A. Dayeh, C. Soci, P. K. L. Yu, E. T. Yu, and D. Wang, “Transport properties of InAs nanowire field effect transistors: The effects of surface states,” *J. Vac. Sci. Technol. B* **25**, 1432 (2007).